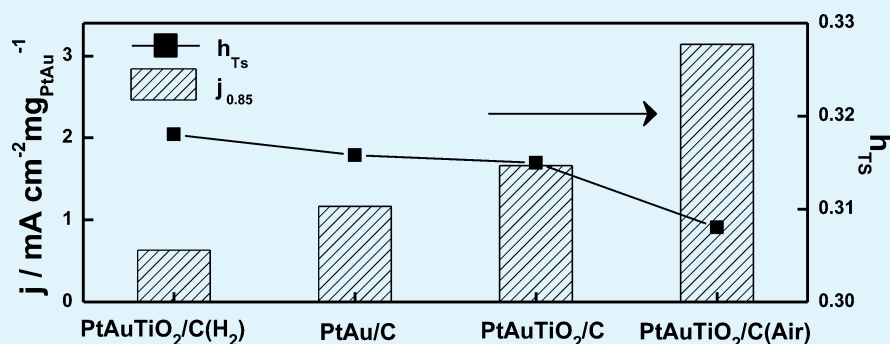# Promotion of Oxygen Reduction Reaction Durability of Carbon-Supported PtAu Catalysts by Surface Segregation and TiO$_2$ Addition

Chen-Wei Liu,[†] Hong-Shuo Chen,[†] Chien-Ming Lai,[‡] Jiunn-Nan Lin,[‡] Li-Duan Tsai,[‡] and Kuan-Wen Wang*,[†]

[†]Institute of Materials Science and Engineering, National Central University, Taoyuan 320, Taiwan

[‡]Material and Chemical Research Laboratories, Industrial Technology Research Institute, Hsinchu 310, Taiwan

S *Supporting Information*

ABSTRACT: Highly effective carbon supported-Pt$_{75}$Au$_{25}$ catalysts for oxygen reduction reaction (ORR) are prepared though titanium dioxide modification and post heat treatment. After accelerated durability test (ADT) of 1700 cycles, the ORR activity of PtAu/C catalysts modified by TiO$_2$ and air heat treatment is 3 times higher than that of the commercial Pt/C. The enhancement of ORR activity is attributed to surface and structural alteration by air-induced Pt surface segregation and lower unfilled d states. On the contrary, for TiO$_2$ modified and H$_2$ treated PtAu/C catalysts, the deterioration of the ORR activity may be due to the loss of electrochemical surface area after ADT and the increase of d-band vacancy.

KEYWORDS: Pt−Au, oxygen reduction reaction (ORR), surface segregation, accelerated durability test (ADT), unfilled d states

1. INTRODUCTION

Although the proton exchange membrane fuel cell (PEMFC) is a kind of promising future power source,[1] the main obstacles for the commercialization of PEMFC are the unsatisfactory long-term durability and the high cost of the cathode catalysts.[2] At present, the carbon-supported platinum (Pt/C) catalysts are generally used as cathode catalysts for oxygen reduction reaction (ORR).[2] However, the carbon corrosion, loss, agglomeration, reduction of electrochemical active surface area (ECSA), and the dissolution of Pt atoms at the carbon support surface cause the serious degradation of Pt/C.[2−6] Therefore, the preparation and modification of cathode catalysts have attracted much attention.[7−10]

Carbon-supported PtAu alloy nanoparticles (NPs) have become promising candidates for the ORR catalysts. The Au atoms alloyed into Pt can modify its electronic state, thereby stabilizing Pt during the long-term measurement.[7] The modification of Pt by Au atoms results in an increase in Pt oxidation potential, which promotes its durability during the ORR measurement. Besides, the incorporation of Au can reduce the local O coverage at high potentials and thus stabilize the Pt surface due to separation and dilution of the active site.[8] On the basis of the X-ray absorption near edge spectroscopy

(XANES) results, Mukerjee et al. have reported that Pt alloy catalysts have better ORR activity than Pt/C due to the increase of d-band vacancy for Pt/C catalyst.[9] Furthermore, previous results are shown that the Pt$_{75}$Au$_{25}$/C alloy catalysts exhibit better ORR performance compared to that with the other bulk compositions, suggesting that the appropriate atomic ratio as well as the surface states of the alloy NPs benefit their catalytic properties.[10]

To further improve the ORR activity and solve the carbon corrosion issues, recent studies have focused on the modification of the support by transition metal oxides, such as TiO$_2$.[11,12] Addition of TiO$_2$ can improve the long-term durability of the Pt/C on the basis of the anchor effect between the metal oxides and the adjacent Pt atoms, and the increase of ECSA.[13−16] Besides, a post-heat treatment applied to the catalysts is an important process to enhance their electro-activity. During the thermal process, the surface reconstruction will happen for alloy catalysts.[17−19] Heat treatments of catalysts in H$_2$ are shown to improve their degree of alloying, stability,

durability, and activity.[17−21] For PtAu/C catalysts, the thermal treatment carried out under H_2/N_2 at 773 K enhances the surface enrichment of Au and alloying degree, suggesting that the surface properties of the catalysts are modified by the thermal treatment.[18] Besides, heat treatments in inert gases such as N_2 or Ar have also been used to remove the residual surfactants, modify the surface chemical states, promote the catalytic activity, and improve the extents of alloying of the alloy NPs.[19−21] For the PtRu/C applied as catalysts for methanol oxidation reaction (MOR), N_2 treatment is used as an adjustment process to tune the surface composition and structure of the alloy NPs and enhance the MOR performance, especially at 570 K.[21]

In this study, we demonstrate a synergistic modification process through TiO_2 addition and post heat treatment to enhance the ORR performance of carbon supported $Pt_{75}Au_{25}$ catalysts. The comparison of the long-term durability of the catalysts is conducted with linear sweep voltammetry (LSV) curve and accelerated durability test (ADT). The surface composition of cathode catalysts is revealed by X-ray photoelectron spectroscopy (XPS). Besides, the d-band vacancy of the prepared catalysts is investigated by XANES.

2. EXPERIMENTAL SECTION

2.1. Preparation of Catalysts. The carbon-supported $Pt_{75}Au_{25}$ alloy catalysts with 35 wt % metal loading and TiO_2 modification are prepared. In the beginning, the desired amounts of titanium isopropoxide dissolved in ethanol were mixed with carbon in a 1:1 ratio at 303 K and finally the hydrolysate was denoted as as-prepared TiO_2/C. Then, aqueous solutions of H_2PtCl_6 (Alfa Aesar) and $HAuCl_4$ (Aldrich) were blended, reduced by isopropyl alcohol (IPA) and codeposited onto the as-prepared TiO_2/C at pH 8 at 343 K. The as-deposited catalysts were subsequently stirred, washed, and dried at 320 K, and denoted as $PtAuTiO_2/C$. For further promotion of the electrochemical performance, the $PtAuTiO_2/C$ catalysts were heat treated for 1 h at 673 K under flowing H_2 or air gas at a flow rate of 50 mL min^{-1}. The alloy catalysts treated in H_2 and air were designated as $PtAuTiO_2/C(H_2)$ and $PtAuTiO_2/C(Air)$, respectively. The Pt/C (46 wt %, TKK, Tanaka Kikinzoku Kogyo), as-prepared PtAu/C and PtAu/C after heat treatment in air at 673 K (35 wt %) were used for comparison. Besides, the as-prepared TiO_2/C supports were heat treated for 1 h at 673 K under flowing H_2 and air gas at a flow rate of 50 mL min^{-1} and named as $TiO_2/C(H_2)$ and $TiO_2/C(Air)$, respectively.

2.2. Characterization of Catalysts. The metal loadings and exact compositions of the catalysts were measured by thermogravimetric analysis (TGA, Perkin-Elmer TGA-7) and inductively coupled plasma-atomic emission spectroscopy (ICP-AES, Jarrell-Ash, ICAP 9000), respectively. Phases and structures of the catalysts were examined by an Shimadzu X-ray diffractometer with a CuK_α (λ = 0.15406 nm) radiation source generated at 40 kV and 25 mA and performed in a 2θ range of 20 and 80°. Scherrer's formula was used to calculate the mean crystallite size of alloy NPs (L_{alloy}).

$$L_{alloy} = \frac{K\lambda}{\text{fwhm} \cos \theta} \tag{1}$$

where λ = 0.154 nm is the wavelength, K = 0.89 is the Scherrer constant, θ is the Bragg angle, and fwhm is the full width at half-maximum.

The morphologies and size distributions of catalysts were characterized by a high-resolution transmission electron microscope (HRTEM, Jeol-2100) with a LaB_6 electron gun source operated at 200 KV. An XPS (Thermo VG Scientific Sigma Probe) using an Al K_α radiation was used to investigate the surface chemical states and compositions of the catalysts. Background removal was performed by a Shirley-type baseline subtraction and then the experimental curve was

fitted by a combination of Lorentzian and Gaussian lines. The binding energy was calibrated with reference to the C1s peak at 284.6 eV.

Electrochemical measurements were conducted by a glassy carbon (GC) rotating disk electrode (RDE), a MSR rotator (Pine Instrument) and a microcomputer-controlled electrochemical analyzer (CHI700a, CH Instrument). A Pt plate and a saturated calomel electrode were used as the counter and reference electrodes, respectively. A 0.5 M H_2SO_4 (Panreac) aqueous solution saturated with high-purified O_2 was used as the electrolyte. The catalysts were dispersed in 2-propanol, blended with diluted Nafion solution (5 wt %, DuPont), and then deposited onto the GC (0.196 cm^2 area). LSV was conducted to study the activity of the ORR with a scan rate of 5 mV s^{-1} and a rotational rate of 1600 rpm. Furthermore, ADT was conducted by continuously potential cycling between 0.6 and 1.2 V with periodic measurements of ECSA and ORR activity after every 200 cycles.

The cyclic voltammograms (CV) characterization on an identical three-electrode system was recorded at a scan rate of 20 mV s^{-1} in the N_2-saturated 0.5 M H_2SO_4 aqueous solution between 0 and 1.2 V. The ECSA was performed by the integration of the charges associated with hydrogen adsorption/desorption region and by the use of assumed value for desorption of monolayer H_{ads} on Pt of near 210 μC cm^{-2}.[22−24] Each ECSA value is normalized to the original active surface area.

The XANES was used to calculate total number of unoccupied d-states (h_{Ts}) for various catalysts. The XANES spectra of various PtAu/C catalysts were measured at the BL01C1 beamline at the National Synchrotron Radiation Research Center. Data were collected at Pt L_{II}-edge (13273 eV) and Pt L_{III}-edge (11563 eV) in fluorescence mode. Catalysts were dispersed uniformly on the tape and prepared as thin pellets with an appropriate absorption thickness.

3. RESULTS AND DISCUSSION

The XRD patterns of as-prepared TiO_2/C, $TiO_2/C(H_2)$ and $TiO_2/C(Air)$ supports are compared in Figure 1a. Besides a
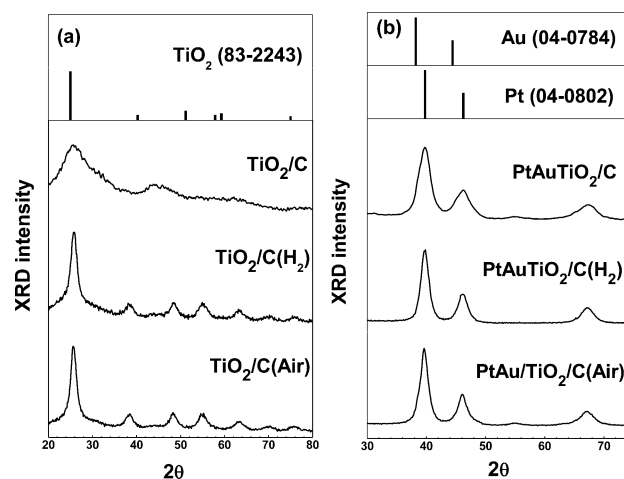

Figure 1. XRD patterns of (a) as-prepared TiO_2/C, $TiO_2/C(H_2)$ and $TiO_2/C(Air)$ supports; and (b) Pt, Au, $PtAuTiO_2/C$, $PtAuTiO_2/C(H_2)$, and $PtAuTiO_2/C(Air)$ catalysts.

strong diffraction peak at 25° from the C support, the diffraction peaks observed at 38.4, 48.2, 54.8, 63.2, and 69.7° for hear-treated supports correspond to TiO_2 (JCPDS 83−2243). Besides, the XRD patterns displayed in Figure 1b show that the grain sizes of PtAu for $PtAuTiO_2/C$, $PtAuTiO_2/C(Air)$ and $PtAuTiO_2/C(H_2)$ catalysts are 3.2, 4.8, and 4.8 nm, respectively. The lattice constant of $PtAuTiO_2/C$, $PtAuTiO_2/C(Air)$ and $PtAuTiO_2/C(H_2)$ is about 0.393 nm, which is consistent with that of PtAu alloy structure.[25] Moreover, no extra peaks related to TiO_2 are detected for the catalysts,

1590

dx.doi.org/10.1021/am404334k | ACS Appl. Mater. Interfaces 2014, 6, 1589−1594

suggesting that TiO_2 may exist as amorphous form or the peak intensity is too weak to be noted.

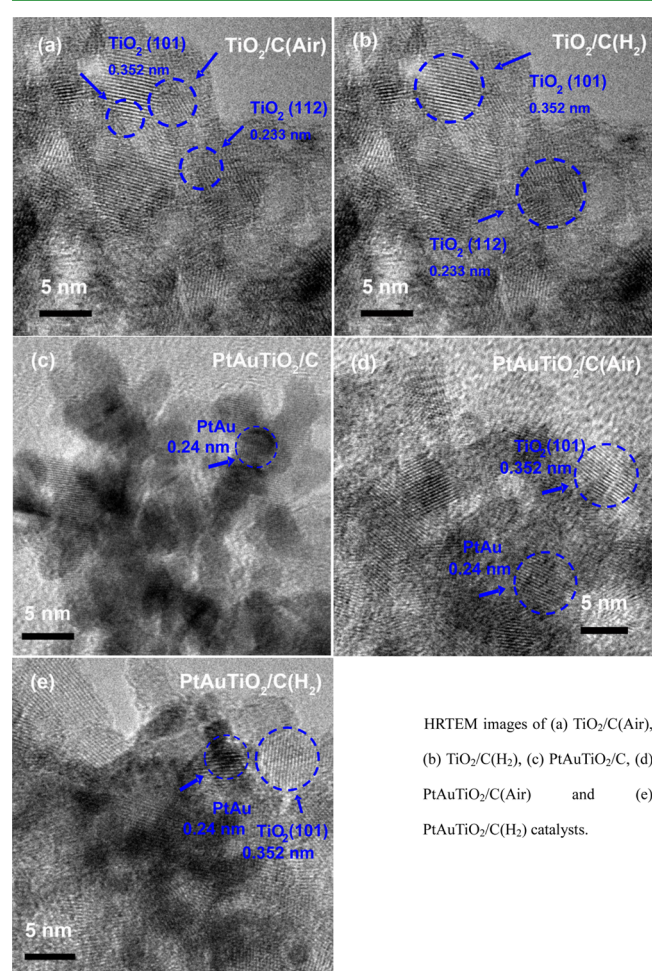Figure 2a−e shows the HRTEM morphologies of TiO_2/C(Air), TiO_2/C(H$_2$), PtAuTiO$_2$/C, PtAuTiO$_2$/C(Air), and

Figure 2. HRTEM images of (a) TiO_2/C(Air), (b) TiO_2/C(H$_2$), (c) PtAuTiO$_2$/C, (d) PtAuTiO$_2$/C(Air), and (e) PtAuTiO$_2$/C(H$_2$) catalysts.

PtAuTiO$_2$/C(H$_2$) samples, respectively. On the basis of the calculation, the interplanar lattice parameters for TiO_2/C(Air) and TiO_2/C(H$_2$) catalysts displayed in images a and b of Figure 2 are equal to 0.233 and 0.352 nm, which is consistent with the (112) and (101) lattice fringe of TiO_2 structure, respectively.[26] Although the XRD patterns of TiO_2/C, TiO_2/C(Air) and TiO_2/C(H$_2$) do not exhibit obvious peaks for TiO_2, TEM results suggest that TiO_2 exists in the vicinity of PtAu NPs. Besides, the lattice fringes of various PtAuTiO$_2$/C catalysts are equal to 0.24 and 0.352 nm, which is consistent with that of PtAu alloy and TiO_2, respectively.[26−28] The particle size of PtAu alloy NPs (d_{PtAu}) calculated from Figure 2c−e for PtAuTiO$_2$/C, PtAuTiO$_2$/C(Air) and PtAuTiO$_2$/C(H$_2$) catalysts and listed in Table 1 is about 3.4, 5.0, and 5.0 nm, respectively, suggesting that the post heat treatment slightly results in the particle growth of the PtAu NPs.

The XPS spectra of various PtAu/C catalysts are displayed in Figure S1 in the Supporting Information and their surface Pt/Au compositions results are listed in Table 1. As compared in Table 1, the surface Au compositions of PtAuTiO$_2$/C,

Table 1. Particle Sizes, Surface Compositions, and ORR Activities of Pt/C, PtAu/C, PtAuTiO$_2$/C, PtAuTiO$_2$/C(Air), and PtAuTiO$_2$/C(H$_2$) catalysts

catalysts	d_{PtAu}(nm)[a]	surface composition (Pt:Au)[b]	ORR activity (at E = 0.85 V) (mA cm^{-2})		
			$I_{0.85-1}$[c]	$I_{0.85-1700}$[d]	MA[e]
Pt/C			0.70	0.07	1.52
PtAu/C	4.6	72:28	0.41	0.02	1.17
PtAuTiO$_2$/C	3.4	86:14	0.58	0.05	1.66
PtAuTiO$_2$/C(H$_2$)	5.0	74:26	0.22	0.01	0.63
PtAuTiO$_2$/C(Air)	5.0	96:4	1.10	0.20	3.14

[a]The particle size of alloy catalysts was calculated from HRTEM image. [b]The surface compositions of the catalysts were estimated by XPS. [c]The current density determined from rotating-disk voltammograms. [d]The current density determined from rotating-disk voltammograms after 1700 cycles. [e]Mass activity (MA): mA cm^{-2} mg^{-1}(PtAu or Pt).

PtAuTiO$_2$/C(Air), and PtAuTiO$_2$/C(H$_2$) are about 14, 4, and 26%, respectively. It can be seen that when compared with PtAuTiO$_2$/C catalysts, the surface Au composition of PtAuTiO$_2$/C(H$_2$) increases from 14 to 26%. According to the literature, the bimetallic PtAu NPs transform to the most stable Pt-core/Au-shell structure from their initial structures when heated at some given temperatures.[28] It means that the surface Au segregation under hear treatment is inevitable during heating. On the contrary, the surface Pt composition of PtAuTiO$_2$/C, PtAuTiO$_2$/C(Air) and PtAuTiO$_2$/C(H$_2$) is about 86, 96, and 74%, respectively, suggesting that Pt atoms segregate to the outmost surface under air treatment dramatically, which is against the prediction and calculation of thermodynamics.[28] It has been proposed that for PtAu catalysts modified by CeO_2 and annealing under N$_2$ at 620 K, the atomic percentage of Pt increases when compared with that of the unmodified PtAu/C because the oxygen atoms released from the CeO_2 oxidize Pt by the reactions[29]

$$CeO_2 \leftrightarrow CeO_{2-x} + x/2O_2 \ (0 \leq x \leq 0.5) \quad (2)$$

$$x/2O_2 + Pt \leftrightarrow Pt^sO_x \quad (3)$$
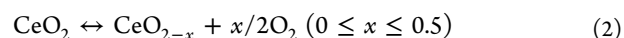
This unexpected Pt surface segregation may be due to the oxidation of Pt on the surface (Pt^s) through oxygen atoms released from CeO_2. The PtAu/C catalysts with Pt surface enrichment consequently have high ORR activity.[29] Therefore, in our research, the surface Pt segregation of PtAuTiO$_2$/C(Air) may be attributed to TiO_2 effect. The heat treatment in air atmosphere causes the release of oxygen atoms from TiO_2 by the reaction

$$TiO_2 \leftrightarrow TiO_{2-x} + x/2O_2 \ (0 \leq x \leq 0.5) \quad (4)$$
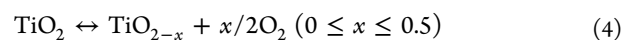
Then, the oxygen may oxidize Pt by eq 3. The oxidation of Pt may drive the significant Pt surface segregation during air heat treatment. In other words, when heating in air, the addition of TiO_2 may cause the oxidation of Pt, which changes the inherent Au segregation property in air. Moreover, through TiO_2 addition and air treatment, the surface energies of Pt and/or Au may be modified. Accordingly, the TiO_2-induced Pt surface segregation and reconstruction takes place, which may further affect their ORR performance. On the other hand, the Pt 4f spectra and the peak fitting results are depicted in Figure S1 in

the Supporting Information. The broad peaks located at about 71 and 74 eV for Pt $4f_{7/2}$ and Pt $4f_{5/2}$, respectively, can be deconvoluted into two set of peaks belonging to Pt and Pt oxides. The peak fitting results listed suggest that the Pt/PtO ratio increases from 83/17 to 87/13 due to TiO_2 addition, and further enhances to 96/4 after heat treatment in air. These results imply that the Pt oxide formation is inhibited in the PtAuTiO$_2$/C(Air) significantly.

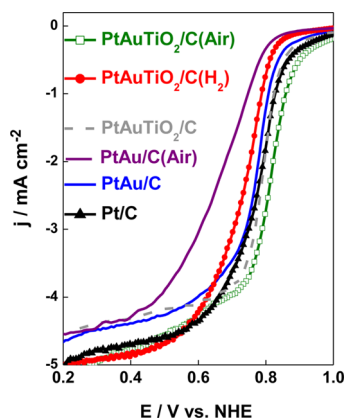Figure 3 compares the LSV for the commercial Pt/C and various PtAu/C catalysts. Table 1 summarizes their current

Figure 3. LSV recorded in 0.5 M H_2SO_4 saturated with O_2 for Pt/C, PtAu/C, PtAu/C(Air), PtAuTiO$_2$/C, PtAuTiO$_2$/C(Air), and PtAu-TiO$_2$/C(H$_2$) catalysts.

densities at $E = 0.85$ V ($I_{0.85}$). As compared to Pt/C, PtAuTiO$_2$/C, and PtAuTiO$_2$/C(H$_2$) catalysts have a negative shift in the onset potential. This deterioration may be due to the depletion of surface Pt and H$_2$-induced Au segregation as listed in Table 1. On the contrary, the ORR activity of PtAuTiO$_2$/C(Air) catalysts exhibits a positive shift in onset potential as well as the current density when compared with Pt/C. The promotional effect of PtAuTiO$_2$/C(Air) catalysts may be related to the surface segregation of Pt as compared in Table 1. Furthermore, the mass ORR activities of various PtAu/C catalysts are compared in Table 1. The mass ORR activity of

the PtAuTiO$_2$/C(Air) catalysts is 2.1 times higher than that of Pt/C. It can be seen that for PtAuTiO$_2$/C(Air), surface enrichment of Pt is favorable to enhance the ORR activity. It is worth mentioning that this ORR promotion is not attributed to the air heat treatment solely, because the ORR performance of PtAu/C(Air) seems to be inferior to that of PtAu/C, confirming that the synergistic effect of TiO_2 addition and air treatment obviously promotes the ORR performance of PtAu/C.

The ADT results compared in Figure 4a and Table 1 also show that after 1700 cycles, the ORR activity of the PtAuTiO$_2$/C(Air) catalysts at 0.85 V is 3.0 times higher than that of the Pt/C. On the contrary, as compared to Pt/C, the ORR activity of PtAu/C, PtAuTiO$_2$/C, and PtAuTiO$_2$/C(H$_2$) catalysts exhibits a dramatic decrease after ADT. Besides the effect of surface Pt depletion, the deterioration may be attributed to the loss of ECSA during long-term measurement, which can be confirmed by ECSA results shown in Figure 4b. However, it seems that the ECSA decay rate of PtAu/C shown in Figure 4b may decrease because of the addition of TiO_2 and can then further decline after heat treatment in air or H$_2$. It suggests that addition of TiO_2 and heat treatment in air may synergistically intensify the interaction between Pt and the support, which may resist the Pt dissolution and migration, and further retain the ECSA during long-term test.

The Pt L_{II} and L_{III}-edges for the various PtAu/C catalysts are characterized by XANES. The normalized absorption at 11564 eV is electronic transition of $2p_{3/2}$ to $5d_{5/2}$ for Pt L_{III}-edge and the intensity of the absorption peak is known as the white line (WL) which represents the orbital occupancy of the 5d electronic state. It has been reported that when compared to the pure Pt catalysts, the enhancement of ORR activity for PtCo/C catalysts is attributed to lower unfilled Pt d-states.[30] The XANES spectrum obtained with various PtAu/C at the Pt L_{III}-edge is depicted in Figure S2 in the Supporting Information. The WL intensity becomes smaller for TiO_2-modified PtAu/C, meaning weaker Pt–O$^-$ bonds and less Pt oxide formation.[32] The decreased Pt oxidation can also be noted from the CV scans exhibited in Figure S3 of the Supporting Information for Pt/C and various PtAu/C. The
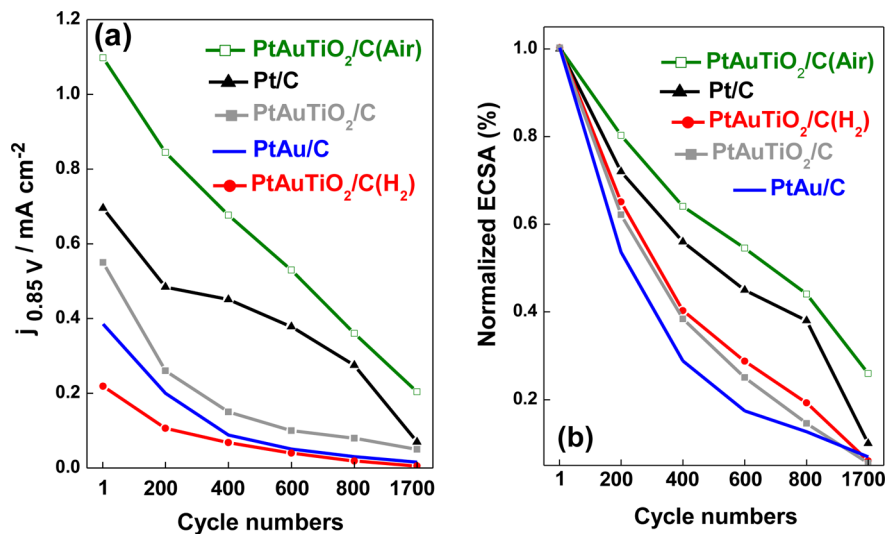

Figure 4. (a) ORR performance and (b) normalized ECSA during 1700 potential cycles of Pt/C, PtAu/C, PtAuTiO$_2$/C, PtAuTiO$_2$/C(Air), and PtAuTiO$_2$/C(H$_2$) catalysts.

higher onset potential of the Pt oxidation at the potential range between 0.7 and 1.1 V indicates the reduced oxidation of PtAu/C, especially TiO₂-modified PtAu/C catalysts.[7] Moreover, based on the Pt L_{III} and L_{II} spectra, the fractional change in the number of d-band vacancies relative to the reference material (f_d) can be estimated according to the following equation[9]

$$f_d = \frac{(\Delta A_3 + 1.11\Delta A_2)}{(A_3 + 1.11A_2)_r} \quad (5)$$

where ΔA_2 and ΔA_3 are expressed by

$$\Delta A_2 = (A_{2s} - A_{2r}) \text{ and } \Delta A_3 = (A_{3s} - A_{3r}) \quad (6)$$

The terms A_2 and A_3, which represent the areas under L_{II} and L_{III} absorption edges of the sample (s) and reference (r) material as well as the calculated the number of unfilled d-states in the sample (h_{Ts}) are evaluated from band structure calculations. The d-band vacancies of Pt in the sample can be evaluated using the following equation.

$$h_{Ts} = (1 + f_d)h_{Tr} \quad (7)$$

The h_{Ts} values of PtAu/C, PtAuTiO₂/C, PtAuTiO₂/C(Air), and PtAuTiO₂/C(H₂) are 0.316, 0.315, 0.308, and 0.318, respectively. The variations in the h_{Ts} of various PtAu catalysts follows the order: PtAuTiO₂/C(Air) < PtAuTiO₂/C< PtAu/C < PtAuTiO₂/C(H₂), which are significantly related to their ORR performance. When compared to PtAu/C, the h_{Ts} of PtAuTiO₂/C is slightly lower, suggesting that addition of TiO₂ partially modifies the electronic state of the PtAu NPs. Moreover, h_{Ts} can be further decreased through the air heat treatment. This result implies that the occupancy in the 5d orbital is decreased and Pt−O⁻ bond strength is weakened because of the synergistic effect of TiO₂ addition and air treatment on the PtAuTiO₂/C(Air) sample.[31,32] However, the calculated h_{Ts} suggests that the PtAuTiO₂/C(H₂) catalysts have a significant increase in the d-band vacancy, resulting in the decline in ORR performance. The correlation between ORR mass activity and h_{Ts} values for various catalysts is compared in Figure 5. The catalyst with the lower h_{Ts} has weaker Pt−O⁻ bonds, less Pt oxide formation, and less pronounced WL, leading to the promotion of ORR kinetics.[32] Therefore, when compared to PtAu/C, PtAuTiO₂/C and PtAuTiO₂/C(H₂) catalysts, the PtAuTiO₂/C(Air) with lower h_{Ts} exhibits better
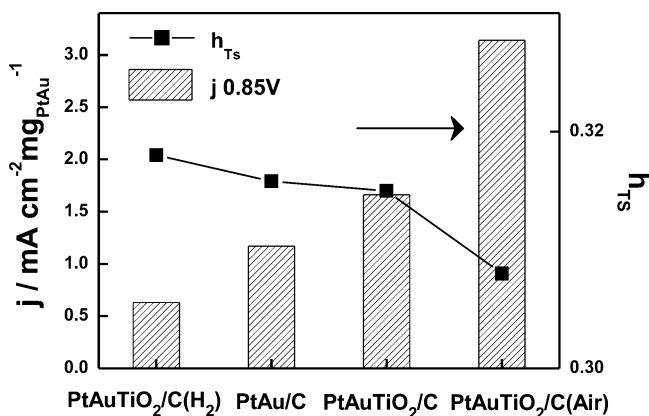
ORR performance because of less Pt-oxide formation and lower Pt−O⁻ bond strength.

4. CONCLUSIONS

Carbon-supported Pt₇₅Au₂₅ alloy catalysts are promoted synergistically by TiO₂ addition and post heat treatment for ORR. After ADT of 1700 cycles, the ORR activity of PtAuTiO₂/C(Air) catalysts is 3 times higher than that of the commercial Pt/C. The enhancement of ORR activity is attributed to the surface enrichment of Pt and lower h_{Ts}. On the contrary, for PtAuTiO₂/C(H₂) catalysts, the deterioration of the ORR activity may be due to the loss of ECSA after ADT and the increase in d-band vacancy.

■ ASSOCIATED CONTENT

ⓢ Supporting Information

XPS, XANES, and CV results. This material is available free of charge via the Internet at http://pubs.acs.org

■ AUTHOR INFORMATION

Corresponding Author

*E-mail: kuanwen.wang@gmail.com.

Notes

The authors declare no competing financial interest.

■ ACKNOWLEDGMENTS

■ REFERENCES

(1) Sarma, L. S.; Chen, C. H.; Kumar, S. M. S.; Wang, G.-R.; Yen, S. C.; Liu, D. G.; Sheu, H. S.; Yu, K. L.; Tang, M. T.; Lee, J. F. *Langmuir* **2007**, *23*, 5802−5809.

(2) Ralph, T.; Hogarth, M. *Platinum Met. Rev.* **2002**, *46*, 117−135.

(3) Ferreira, P. J.; la O', G. J.; Shao-Horn, Y.; Morgan, D.; Makharia, R.; Kocha, S.; Gasteiger, H. A. *J. Electrochem. Soc.* **2005**, *152*, A2256−A2271.

(4) Antolini, E. *J. Mater. Sci.* **2003**, *38*, 2995−3005.

(5) Blurton, K.; Kunz, H.; Rutt, D. *Electrochimi. Acta* **1978**, *23*, 183−190.

(6) Zhai, Y.; Zhang, H.; Xing, D.; Shao, Z. G. *J. Power Sources* **2007**, *164*, 126−133.

(7) Zhang, J.; Sasaki, K.; Sutter, E.; Adzic, R. R. *Science* **2007**, *315*, 220−222.

(8) Fang, Y. H.; Liu, Z.-P. *J. Phys. Chem. C* **2011**, *115*, 17508−17515.

(9) Mukerjee, S.; Srinivasan, S.; Soriaga, M. P.; McBreen, J. *J. Electrochem. Soc.* **1995**, *142*, 1409−1422.

(10) Liu, C. W.; Wei, Y. C.; Wang, K. W. *J. Colloid Interface Sci.* **2009**, *336*, 654−657.

(11) Liu, X.; Chen, J.; Liu, G.; Zhang, L.; Zhang, H.; Yi, B. *J. Power Sources* **2010**, *195*, 4098−4103.

(12) Huang, K.; Sasaki, K.; Adzic, R. R.; Xing, Y. *J. Mater. Chem.* **2012**, *22*, 16824−16832.

(13) Liu, G.; Zhang, H.; Zhai, Y.; Zhang, Y.; Xu, D.; Shao, Z. G. *Electrochem. Commun.* **2007**, *9*, 135−141.

(14) Kim, D. S.; Kwak, S.-Y. *Appli. Catal. A: General* **2007**, *323*, 110−118.

(15) Sathiyanarayanan, S.; Azim, S. S.; Venkatachari, G. *Electrochimi. Acta* **2007**, *52*, 2068−2074.

(16) Shim, J.; Lee, C. R.; Lee, H. K.; Lee, J. S.; Cairns, E. J. *J. Power Sources* **2001**, *102*, 172−177.

(17) Sarkar, A.; Murugan, A. V.; Manthiram, A. *J. Phys. Chem. C* **2008**, *112*, 12037−12043.

Figure 5. Correlation between ORR mass activity and h_{Ts} values for PtAu/C, PtAuTiO₂/C, PtAuTiO₂/C(Air), and PtAuTiO₂/C(H₂) catalysts.

1593

dx.doi.org/10.1021/am404334k | *ACS Appl. Mater. Interfaces* 2014, 6, 1589−1594

(18) Liu, C. W.; Wei, Y. C.; Wang, K. W. *Chem. Commun.* **2010**, *46*, 2483−2485.

(19) Wei, Y. C.; Liu, C. W.; Wang, K. W. *ChemPhysChem* **2009**, *10*, 1230−1237.

(20) Li, X.; Hsing, I. M. *Electrochimi. Acta* **2006**, *52*, 1358−1365.

(21) Wei, Y. C.; Liu, C. W.; Chang, W. J.; Wang, K. W. *J. Alloys Compd.* **2011**, *509*, 535−541.

(22) Pozio, A.; De Francesco, M.; Cemmi, A.; Cardellini, F.; Giorgi, L. *J. Power Sources* **2002**, *105*, 13−19.

(23) Ticianelli, E.; Beery, J.; Srinivasan, S. *J. Appl. Electrochem.* **1991**, *21*, 597−605.

(24) Antolini, E.; Giorgi, L.; Pozio, A.; Passalacqua, E. *J. Power Sources* **1999**, *77*, 136−142.

(25) Chen, J.; Herricks, T.; Geissler, M.; Xia, Y. *J. Am. Chem. Soc.* **2004**, *126*, 10854−10855.

(26) Huang, K.; Sasaki, K.; Adzic, R. R.; Xing, Y. *J. Mater. Chem.* **2012**, *22*, 16824−16832.

(27) Choi, J. H.; Park, K. W.; Park, I. S.; Kim, K.; Lee, J. S.; Sung, Y. E. *J. Electrochem. Soc.* **2006**, *153*, A1812−A1817.

(28) Liu, H.; Pal, U.; Ascencio, J. *J. Phys. Chem. C* **2008**, *112*, 19173−19177.

(29) Liu, C. W.; Wei, Y. C.; Wang, K. W. *J. Phys. Chem. C* **2011**, *115*, 8702−8708.

(30) Lai, F. J.; Sarma, L. S.; Chou, H.-L.; Liu, D. G.; Hsieh, C.-A.; Lee, J.-F.; Hwang, B.-J. *J. Phys. Chem. C* **2009**, *113*, 12674−12681.

(31) Lai, F. J.; Su, W. N.; Sarma, L. S.; Liu, D. G.; Hsieh, C. A.; Lee, J. F.; Hwang, B. J. *Chem.—Eur. J.* **2010**, *16*, 4602−4611.

(32) Yeh, T.-H.; Liu, C.-W.; Chen, H.-S.; Wang, K. W. *Electrochem. Commun.* **2013**, *31*, 125−128.